Supplementary Information

Experimental and computational investigation of heat transfer in a microwave-assisted flow system

Spyridon Damilos[1], Anand N. P. Radhakrishnan[1], Georgios Dimitrakis[2], Junwang Tang[1] and Asterios Gavriilidis[1]

[1]*Department of Chemical Engineering, University College London, Torrington Place, London, WC1E 7JE, United Kingdom*

[2]*Department of Chemical and Environmental Engineering, Faculty of Engineering, University of Nottingham, University Park, Nottingham, NG7 2RD, United Kingdom*

Contents

1. Dielectric properties of water

1.1 Measurement of dielectric properties at atmospheric pressure

The relative complex permittivity of water, $\varepsilon_r = \varepsilon' - \varepsilon'' j$ (dielectric constant: ε' and dielectric loss: ε''), was evaluated experimentally between 20-95 ^{o}C and atmospheric pressure, as bubbling occurred above 95 ^{o}C. A coaxial dielectric probe (87070E, Agilent Technologies) connected to a network analyser (PNA-L, Agilent Technologies) was inserted in a 100 ml water sample. E-cal software (Agilent Technologies) was used for the calculation of the dielectric properties at a frequency span of 1-10 GHz (Table S1).

Table S1. Experimental measurements of the relative complex permittivity of ultra-pure water for different temperatures at atmospheric pressure at 2.45 GHz frequency using a coaxial probe, following the methodology described by Robinson et al. [1].

Temperature, T (^{o}C)	**Relative complex permittivity, ε_r (-)**
20	78.6 - 10.5j
25	77.3 - 9.4j
30	76.2 - 8.6j
35	74.6 - 7.5j
40	73.0 - 6.7j
45	71.7 - 6.2j
50	70.6 - 5.8j
55	69.4 - 5.4j
60	68.0 - 5.0j
65	65.9 - 4.5j
70	64.2 - 4.2j
75	63.0 - 4.0j
80	61.8 - 3.9j
85	60.5- 3.7j
90	59.3- 3.5j
95	59.2- 3.4j

1.2 Calculation of dielectric properties as a function of temperature and pressure

In order to model the system at elevated pressures, we investigated the effect of pressure on the water dielectric properties. Table S2 shows the dielectric properties of water calculated from literature empirical correlations. Based on the comparison of the two correlations considered, there is no significant increase of the dielectric constant by increasing the system pressure from 1 bara to 2.3 bara, at different temperatures.

Table S2. Calculated dielectric constant of water at 1 bara and 2.3 bara and at various temperatures, based on the empirical correlations of Bradley & Pitzer [2] and Floriano & Nascimento [3].

Temperature	System pressure	*Bradley & Pitzer*	*Floriano & Nascimento*
0 °C	1 bara	87.57	87.78
	2.3 bara	87.57	87.79
25 °C	1 bara	78.05	78.45
	2.3 bara	78.05	78.45
50 °C	1 bara	69.46	69.91
	2.3 bara	69.46	69.91
75 °C	1 bara	61.74	62.24
	2.3 bara	61.74	62.25

To the best of our knowledge, there are no experimental data of the dielectric constant and dielectric loss of water at 2.3 bara. The boiling point of water at this pressure is 125 °C; thus, as shown on Figure S1, we extrapolated the experimentally measured dielectric properties from Table S1 up to 120 °C since bubbling was observed above that temperature, while the dielectric loss was assumed equal to zero at 125 °C due to the phase change. A linear interpolation was then performed between ε'' at 120 °C to $\varepsilon'' = 0$ at 125 °C by COMSOL.

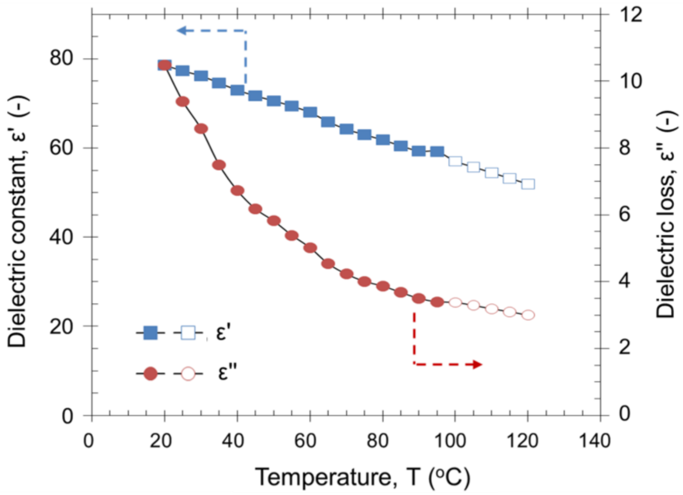

Figure S1. Experimentally measured dielectric properties of water at atmospheric pressure (filled marks) and the extrapolated values (empty marks) for the estimation of the dielectric properties at 2.3 bara pressure (water boiling point at 2.3 bara is 125 °C). Lines are used for visualisation.

2. Effect of fibre optic probe inside the tube

The effect of the fibre optic probe inside the tube was evaluated prior to the parametric investigation of the operational parameters on the temperature profile. Our study simulated the electric field (Figure S2) and the temperature profile (Figure S3) in the tube and the support structure with and without the fibre optic temperature probe, using COMSOL Multiphysics. The probe was positioned at the 5 points for temperature measurements by inserting it from the tube outlet, while in all cases the water flow rate was 0.7 ml/min. The fibre optic probe was considered as a solid cylinder of glass of ~ 1.7 mm diameter ($\varepsilon_{r,glass} = 4.6 - 0.01j$, $C_{p,glass} = 840$ J/kg·K) [1, 4].

The electric field intensity at the measurement points was different in the presence or absence of the fibre optic probe. When the fibre optic probe was at point 3, the electric field intensity on the tip was $1.03 \cdot 10^4$ V/m, while the intensity at the same position without the probe was ~ $0.56 \cdot 10^4$ V/m. These results are in accordance with previous studies in batch vessels, discussing the influence of fibre optic probe in microwave-assisted studies [5]. However, the simulated temperatures at the temperature measurement points were similar in the presence or absence of the probe, similar to the study by Robinson et al. [1]. The negligible temperature difference with or without the inserted fibre optic showed that heat was dissipated uniformly in the medium, despite the local heating of the tip of the probe.

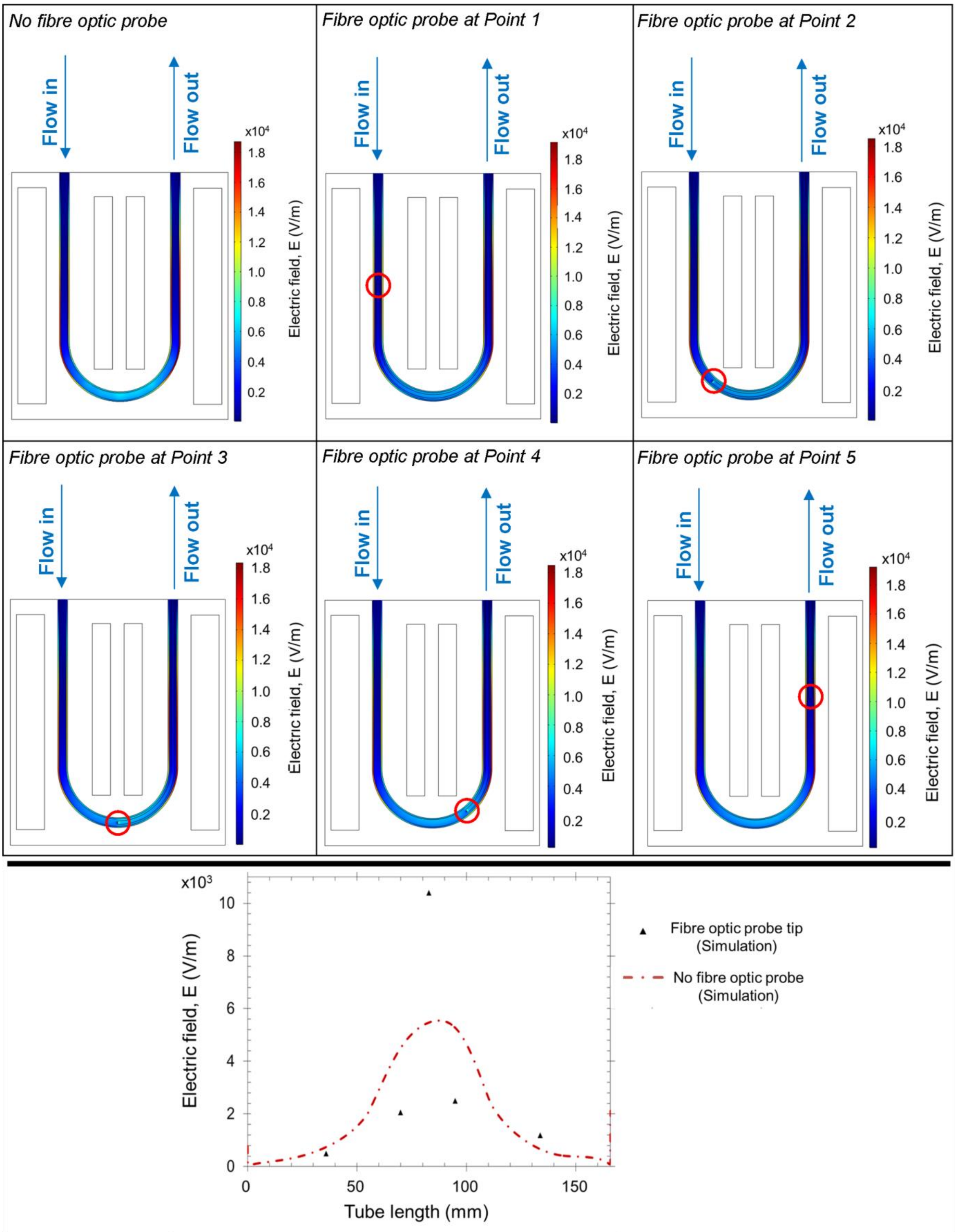

Figure S2. Top: Computational results of the electric field profile inside the U-shape tube without the fibre optic temperature probe and with the probe positioned at the 5 points for temperature measurements by inserting the probe from the tube outlet (point 1: 36 mm, point 2: 70 mm, point 3: 83 mm, point 4: 95 mm, point 5: 135 mm from tube inlet). The tip of the fibre optic probe is noted with a red circle. Bottom: Simulated electric field profile over the tube length without the fibre optic probe (dash-dotted line) and at the measurement points when the fibre optic probe was included in the simulations (triangle marks). Microwave power, 35 W; frequency, 2.45 GHz; flow rate, 0.7 ml/min; tube orientation: parallel-to-port; system pressure, 1 bara.

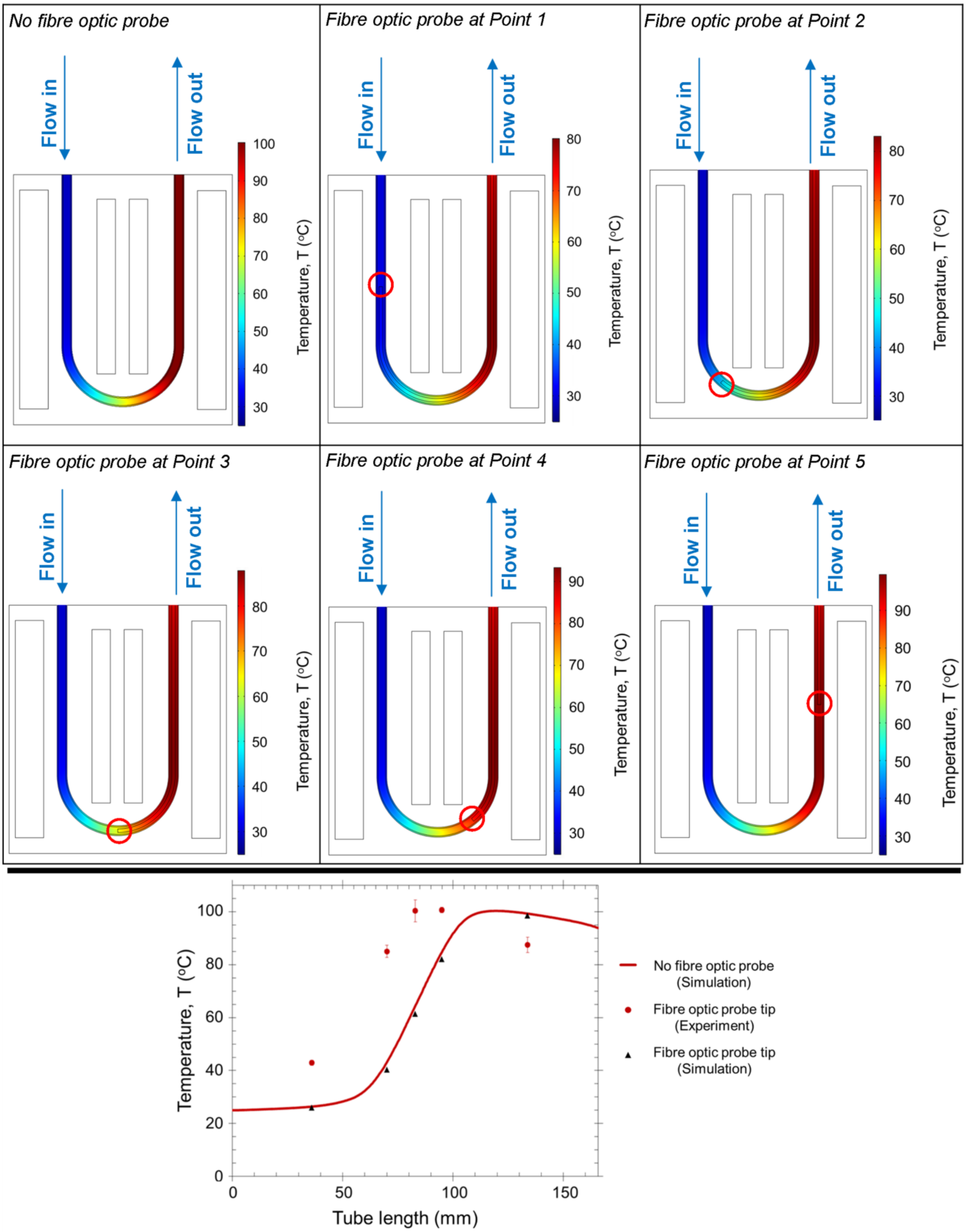

Figure S3. Top: Computational results of the temperature profile inside the U-shape tube without the fibre optic temperature probe and with the probe positioned at the 5 points for temperature measurements by inserting the probe from the tube outlet (point 1: 36 mm, point 2: 70 mm, point 3: 83 mm, point 4: 95 mm, point 5: 135 mm from tube inlet). The tip of the fibre optic probe is noted with a red circle. Bottom: Experimental (circle marks) and simulated temperature profile along the tube length without the fibre optic probe (solid line) and at the measurement points when the fibre optic probe was included in the simulations (triangle marks). Microwave power, 35 W; frequency 2.45 GHz; flow rate, 0.7 ml/min; tube orientation: parallel-to-port; system pressure, 1 bara.

3. COMSOL model description

For the evaluation of the electric field and temperature profiles throughout the tube length and the absorbed microwave power by the flowing water, a FEM model was developed in COMSOL Multiphysics consisting of two steps, Step 1 and Step 2. In Step 1, the electric field inside the microwave cavity was evaluated via the *Electromagnetic Waves, Frequency Domain* module. Step 1 included six domains (the metal cavity, the contained PTFE protective ring, the air, the PTFE support structure, the PTFE tube and the water flowing inside the tube). In Step 2, the temperature profile in the water was evaluated by coupling the *Heat Transfer* and *Laminar Flow* modules. Step 2 included three domains (the PTFE support structure, the PTFE tube and the water).

Step 1

In Step 1 of COMSOL Multiphysics simulation, the following assumptions were made:

- The dielectric properties of air and PTFE were constant
- The microwave energy absorbed by the air was negligible

Model equations

- Time-harmonic electromagnetic field distribution in the metal cavity, PTFE protective ring, air, PTFE support structure, PTFE tube and water domains :

$$\nabla \times \mu_r^{-1}(\nabla \times \boldsymbol{E}) - k_o^2 \varepsilon_r \boldsymbol{E} = 0 \qquad \text{(S-1)}$$

where $k_o = \omega\sqrt{(\varepsilon_o \mu_o)} = \frac{\omega}{c}$ is the wave number of free space, ε_o is the permittivity of free space, μ_0 is the permeability of the free space, ω is the angular frequency, c is the speed of light in the free space, μ_r is the relative permeability, ε_r is the relative permittivity, and $\boldsymbol{E}$ is the electric field vector. Maximum element size in free space was set at 0.0244 m (1/5 of the electromagnetic wavelength in vacuum).

Model boundary conditions

- The inside surfaces of the waveguide were assumed to behave as perfect electric conductor:

  $\boldsymbol{n} \times \boldsymbol{E} = 0$, on the inside waveguide surfaces
- The electric field excitation at the magnetron port is given by:

  $E_z = \left(\sqrt{\frac{4Z_{TE}P_{in}}{A}}\right) sin\left(\frac{\pi y}{L_y}\right)$, normal to the magnetron port

Here, $\boldsymbol{n}$ is the normal vector, the x-direction is normal to the port, the y-direction is parallel to the port width and the z-direction is parallel to the port height, L_y is the dimension of the broad side of the launching waveguide section, A is the area of the launching waveguide section (magnetron port dimensions are 44 mm x 87 mm), P_{in} the input microwave power and $Z_{TE} = \frac{\lambda_g}{\lambda}\sqrt{\frac{\mu_r \cdot \mu_0}{\varepsilon_r \cdot \varepsilon_0}}$ is the wave impedance; the last parameter depends on the properties of the material ($\lambda = {}^{c}/_{f}$ and λ_g are the wavelengths of microwaves in free space and rectangular waveguide, respectively and f the operating microwave frequency). Based on its dimensions, the waveguide is defined as TE_{10} mode [4] translating to transverse electric (TE) waves that have no electric field component in the propagating direction. In this case the wavelength in the rectangular waveguide is given by $\lambda_g = \frac{\lambda}{\sqrt{1-\left({}^{\lambda}/_{L_y}\right)^2}}$.

Step 2

In Step 2 of COMSOL Multiphysics simulation, the following assumptions were made:

- The thermal conductivity of the PTFE was constant
- Water was assumed as incompressible fluid

Model equations

- Energy balance in the water domain:

$$\rho_{water} C_{p,water} (\boldsymbol{u} \cdot \nabla T_{water}) = k_{water} \nabla^2 T_{water} + P_d \tag{S-2}$$

where the microwave power density in water is given by:

$$P_d = 2\pi f \varepsilon_o \varepsilon''_{water} |\boldsymbol{E}|^2 \tag{S-3}$$

- Energy balance in the PTFE tube and support structure domains:

$$k_{PTFE} \nabla^2 T_{PTFE} = 0 \tag{S-4}$$

- Momentum balance in the water domain:

$$\rho_{water} [\boldsymbol{u} \cdot \nabla \boldsymbol{u}] - \eta_{water} \nabla \cdot [\nabla \boldsymbol{u} + (\nabla \boldsymbol{u})^T] + \nabla p = 0 \tag{S-5}$$

- Continuity equation in the water domain:

$$\rho_{water} (\nabla \cdot \boldsymbol{u}) = 0 \tag{S-6}$$

where ε_o is the permittivity of free space, ε'' is the dielectric loss factor, f is the operating microwave frequency, $|\boldsymbol{E}|$ is the electric field intensity, ρ is the density, C_p is the specific heat capacity, k is the thermal conductivity, $\boldsymbol{u}$ is the water velocity field vector inside the tube, η is the dynamic viscosity, p is the pressure and T is the temperature.

Model boundary conditions

- The water temperature at the tube inlet was set as:
  $T_{water} = T_0$, at tube inlet
- No heat flux was assumed at the tube outlet:
  $-\boldsymbol{n} \cdot k_{water} \nabla T_{water} = 0$, at tube outlet
- The heat flux at the interface between the water and the PTFE tube were matched:
  $k_{water} \nabla T_{water} = k_{PTFE} \nabla T_{PTFE}$, at inner tube wall

- The temperature at the interface between the water and the PTFE tube were matched:

  $T_{water} = T_{PTFE}$, at inner tube wall
- The heat loss from the PTFE wall and support structure to the ambient environment due to natural convection and radiation was given by:

  $-\boldsymbol{n} \cdot k_{PTFE} \nabla T_{PTFE} = h_{air}(T_{air} - T_{PTFE}) + \varepsilon_{PTFE}\sigma\left({T^4}_{air} - {T_{PTFE}}^4\right)$, at PTFE surface
- The water velocity at the tube inlet was set as:

  $\boldsymbol{u} = u_0$, at tube inlet
- No slip condition was assumed at the inside walls of the tube:

  $\boldsymbol{u} = 0$, at inner tube wall
- The relative pressure was assumed to be zero at the tube outlet :

  $p_0 = 0$, at tube outlet

Here, $\boldsymbol{n}$ is the normal vector and p_0 is the relative pressure. Input parameters for the COMSOL model (for Step 1 and Step 2) are given in Table S3 and the thermal properties of water are given in Table S4.

Table S3. Input parameters for the COMSOL model (Step 1 and Step 2).

Symbol	**Value**	**Unit**	**Description**
		Step 1	
c	$2.998 \cdot 10^{9}$	m/s	Speed of light in free space
f	$2.45 \cdot 10^{9} – 2.47 \cdot 10^{9}$	Hz	Frequency in the microwave cavity
L_{tube}	$166 \cdot 10^{-3}$	m	Tube length
P_{in}	5 – 35	W	Input microwave power
ε_o	$8.854 \cdot 10^{-12}$	F/m	Permittivity of free space
ε'_{water}	78.6	-	Dielectric constant of water at 20 ^{o}C
ε''_{water}	10.5	-	Dielectric loss of water at 20 ^{o}C
ε'_{PTFE}	2.1	-	Dielectric constant of PTFE
ε''_{PTFE}	0	-	Dielectric loss of PTFE
ε'_{air}	1	-	Dielectric constant of air
ε''_{air}	0	-	Dielectric loss of air
μ_o	$4\pi \cdot 10^{-7}$	H/m	Permeability of free space
$\mu_{r,water}$	1	-	Relative permeability of water
$\mu_{r,PTFE}$	1	-	Relative permeability of PTFE
$\mu_{r,air}$	1	-	Relative permeability of air

Table S3 continued

Symbol	**Symbol**	**Symbol**	**Symbol**
		Step 2	
$C_{p,water}$	see Table S4	J/kg·K	Heat capacity of water
h_{air} [6]	5	W/m^2·K	Heat transfer coefficient of air
k_{PTFE}	0.24	W/m·K	Thermal conductivity of PTFE
k_{water}	see Table S4	W/m·K	Thermal conductivity of water
L_{tube}	166·10^{-3}	m	Tube length
V_{in}	0.5 – 1.5	cm^3/min	Inlet flow rate
R_{tube}	1.2·10^{-3}	m	Tube inner radius
T_0	20	^{o}C	Water temperature at the tube inlet
u_0	1.84 – 5.53	mm/s	Water inlet velocity
ε_o	8.854·10^{-12}	F/m	Permittivity of free space
ε_{PTFE} [7]	0.92	-	Surface emissivity of PTFE
ε'_{water}	see Table S1, Figure S1	-	Dielectric constant of water
ε''_{water}	see Table S1, Figure S1	-	Dielectric loss of water
η_{water}	see Table S4	Pa·s	Dynamic viscosity of water
ρ_{water}	see Table S4	kg/m^3	Density of water
σ	5.6704·10^{-8}	W/m^2·K^4	Stefan-Boltzmann constant

Table S4. Thermal properties of water for the COMSOL model (Step 2).

Density [8]:	$-0.0031\mathrm{T}^2 + 1.5392\mathrm{T} + 810.7$ (kg/m^3)
Dynamic viscosity [9]:	$10^{\left(-0.00001599\mathrm{T}^2+0.021641\mathrm{T}+\left(\frac{1949}{\mathrm{T}}\right)-14.62\right)}$ (Pa·s)
Heat capacity [8]:	$-0.00009\mathrm{T}^3 + 0.1054\mathrm{T}^2 - 39.619\mathrm{T} + 9021.6$ (J/kg·K)
Thermal conductivity [9]:	$-0.0000056209\mathrm{T}^2 + 0.0047054\mathrm{T} - 0.2987$ (W/m·K)

Temperature range: 293.15 – 373.15 K; Temperature in K.

4. References

[1] J. Robinson, S. Kingman, D. Irvine, P. Licence, A. Smith, G. Dimitrakis, D. Obermayer, C.O. Kappe, Understanding microwave heating effects in single mode type cavities-Theory and experiment, Phys Chem Chem Phys 12 (2010) 4750-4758.

[2] D.J. Bradley, K.S. Pitzer, Thermodynamics of electrolytes. 12. Dielectric properties of water and Debye-Hueckel parameters to 350 ^{o}C and 1 kbar, The Journal of Physical Chemistry 83 (1979) 1599-1603.

[3] W.B. Floriano, M.A.C. Nascimento, Dielectric constant and density of water as a function of pressure at constant temperature, Brazilian Journal of Physics 34 (2004) 38-41.

[4] G.S.J. Sturm, M.D. Verweij, T. Van Gerven, A.I. Stankiewicz, G.D. Stefanidis, On the effect of resonant microwave fields on temperature distribution in time and space, International Journal of Heat and Mass Transfer 55 (2012) 3800-3811.

[5] R. Cherbański, L. Rudniak, Modelling of microwave heating of water in a monomode applicator – Influence of operating conditions, International Journal of Thermal Sciences 74 (2013) 214-229.

[6] S. Curet, F. Bellincanta Begnini, O. Rouaud, L. Boillereaux, Modeling microwave heating during batch processing of liquid sample in a single mode cavity, COMSOL ConferenceGrenoble, 2015, pp. 1-16.

[7] Engineering ToolBox (2003), Emissivity coefficients materials. [online] Available at: https://www.engineeringtoolbox.com/emissivity-coefficients-d_447.html [Accessed 27 February 2019].

[8] R.H. Perry, D.W. Green, J.O. Maloney, Perry's Chemical Engineers' Handbook, 7th ed., McGraw-Hill, New York, 1999.

[9] C.L. Yaws, Transport Properties of Chemicals and Hydrocarbons, 2nd ed., Gulf Professional Publishing, Oxford, 2014.